

Continuous Flow Synthesis of Nitrofuran Pharmaceuticals Using Acetyl Nitrate

Hubert Hellwig, Loïc Bovy, Kristof Van Hecke, Cornelis P. Vlaar, Rodolfo J. Romañach, Md. Noor-E-Alam, Allan S. Myerson, Torsten Stelzer, and Jean-Christophe M. Monbaliu*

Abstract: Nitrofurfural is a key building block for the synthesis of antimicrobial nitrofurans as active pharmaceutical ingredients. Its synthesis involves the nitration of furfural, a substrate derived from biobased resources. However, furfural has a delicate heteroaromatic backbone. Typical nitrations involve harsh reaction conditions, which often compromise this structure, resulting in poor reproducibility and low yields. Although acetyl nitrate, a mild nitrating agent, is suitable for this task, major deterrents remain. First, its conventional preparation method involves conditions that are not compatible with furfural. Second, significant safety concerns are associated with the unstable and explosive nature of acetyl nitrate. These critical issues are addressed herein. A safe and robust continuous flow platform featuring *in situ* generation of acetyl nitrate for the nitration of furfural to nitrofurfural is reported. The high level of integration and automation enables remote process operation by a single operator. Key furfural-based pharmaceutical intermediates were synthesized with favorable metrics and high reproducibility. The efficiency of this flow platform is demonstrated using a selection of best-selling nitrofuran pharmaceuticals (nifuroxazide, nifurtimox, nitrofurantoin, and nitrofural), which were obtained with excellent isolated yields in under five minutes.

Introduction

The discovery of aromatic nitration using nitric acid in the early 1830s quickly became a cornerstone of organic chemistry, leading to broad industrial implementation.^[1-4] Nitration reactions are inherently hazardous, often described as the most widespread and powerfully destructive industrial unit process operation. These reactions pose significant risks: they are highly exothermic and prone to thermal runaway, while many nitration (by)products themselves are also classified as potential explosives.^[5,6] This has led to a particular interest in adopting inherently safer technologies, such as flow chemistry, to carry out nitrations.^[7-12] Numerous nitrating

cocktails have been developed, each tailored to accommodate specific substrate reactivity or sensitivity (Figure 1a).^[13] Electron-rich aromatic substrates can undergo nitration with mild reagents, while deactivated aryls require harsher conditions. Heteroaromatics are usually far less resilient owing to their lower aromaticity, often resulting in oxidation, ring opening, polymerization, or other side reactions.^[14]

Among heteroaromatics of wide industrial interest, furfural (2-furaldehyde, **1**) is a furan-derived substrate sourced from biomass waste.^[17,18] Its interest as a pivotal heteroaromatic building block increased after addition in 2010 by the US Department of Energy (DOE) to a list of industrially relevant biobased platform chemicals.^[19] The

[*] Dr. H. Hellwig, L. Bovy, Prof. Dr. J.-C. M. Monbaliu
Center for Integrated Technology and Organic Synthesis (CiTOS),
MolSys Research Unit, University of Liège, B6a, Room 3/19, Allée du
Six Août 13, Liège (Sart Tilman) B-4000, Belgium

E-mail: jc.monbaliu@uliege.be

Prof. Dr. K. Van Hecke

Department of Inorganic and Physical Chemistry, Ghent University,
Krijgslaan 281-S3, Ghent B-9000, Belgium

Prof. Dr. C. P. Vlaar, Prof. Dr. T. Stelzer

Department of Pharmaceutical Sciences, University of Puerto
Rico-Medical Sciences Campus, San Juan, PR 00936, USA

Prof. Dr. R. J. Romañach

Department of Chemistry, University of Puerto Rico – Mayagüez,
Mayagüez, PR 00681, USA

Prof. Dr. M. Noor-E-Alam

Department of Mechanical and Industrial Engineering, College of
Engineering, Center for Health Policy and Healthcare Research,
Northeastern University, Boston, MA 02115, USA

Prof. Dr. A. S. Myerson, Prof. Dr. T. Stelzer

Department of Chemical Engineering, Massachusetts Institute of
Technology, Cambridge, MA 02139, USA

Prof. Dr. T. Stelzer

Crystallization Design Institute, Molecular Sciences Research Center,
University of Puerto Rico, San Juan, PR 00926, USA

Prof. Dr. J.-C. M. Monbaliu

WEL Research Institute, Avenue Pasteur 6, Wavre B-1300, Belgium

Homepage: <https://www.citos.uliege.be>

Additional supporting information can be found online in the
Supporting Information section

© 2025 The Author(s). *Angewandte Chemie International Edition* published by Wiley-VCH GmbH. This is an open access article under the terms of the [Creative Commons](#)

[Attribution-NonCommercial-NoDerivs](#) License, which permits use and distribution in any medium, provided the original work is properly cited, the use is non-commercial and no modifications or adaptations are made.

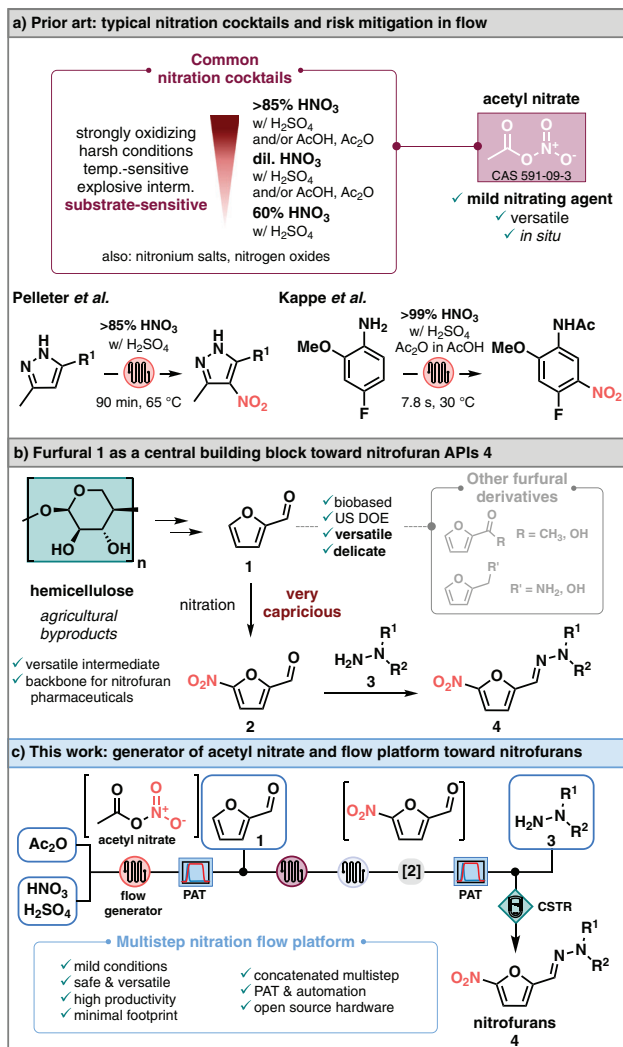


Figure 1. Overall context and strategy. a) Common nitration cocktails^[13] and risk mitigation in flow with selected examples.^[15,16] b) Biobased furfural **1** is derived from hemicellulose and can be used to access important pharmaceutical building blocks. c) To address the capricious nitration of **1**, a concatenated and automated flow platform is developed, featuring an in-line generator of acetyl nitrate.

nitration product of furfural (5-nitrofurfural, **2**) is a key intermediate in the preparation of nitrofurans **4**, a family of active pharmaceutical ingredients (APIs) with antimicrobial properties (Figure 1b).^[20] However, the nitration of **1** is notoriously challenging due to its fragile nature and inability to withstand typical harsh nitrating agents.^[14]

Acetyl nitrate (Figure 1a) is among the milder nitrating reagents compatible with **1**. Reports about its generation go back as far as 1884, while its use for the nitration of **1** in batch dates back to at least 1902.^[21,22] Despite being categorized as mild,^[23] acetyl nitrate is highly sensitive and can explode at temperatures as low as 60 °C.^[5,23] While the ex situ preparation of acetyl nitrate is considered too dangerous,^[23,24] in situ preparation in batch became a privileged alternative. However, in situ generation of acetyl nitrate exposes delicate substrates, such as **1**, to harsh conditions. Solutions to address

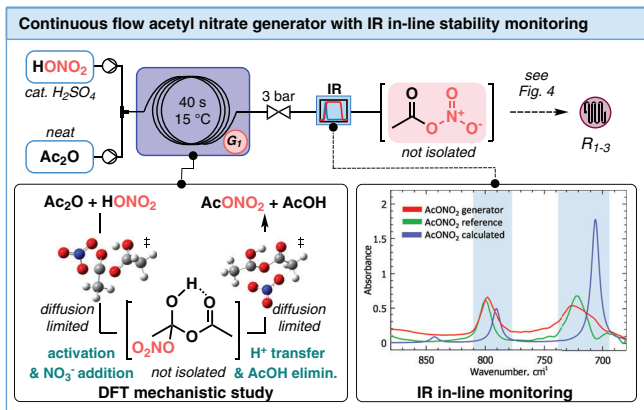


Figure 2. Simplified chart for the acetyl nitrate flow generator (details in Section S6, Supporting Information). Lower left insert: results from the Density Functional Theory (DFT) mechanistic study (Gaussian 16,^[31] B3LYP-GD3B/6-31+G*/M08HX/6-31++G** level of theory, SMD = acetic anhydride at 273 K, Section S8, Supporting Information). Lower right insert: in-line FTIR spectra of acetyl nitrate prepared in flow, according to a reference protocol from silver nitrate and acetyl chloride,^[22] and with results from ground state frequency DFT calculations (Section S8, Supporting Information).

these issues associated with its generation and use for the production of **2** are described here (Figure 1c).

We report a highly automated continuous flow system featuring an acetyl nitrate generator, subsequent nitration of **1**, and a downstream synthesis of nitrofuran pharmaceuticals. Safety is ensured by avoiding the handling of reactive species and intermediates.^[25] The system features technical innovations such as a dedicated filtration and separation unit, and a variety of sensors and Process Analytical Technology (PAT) tools placed at critical points, ensuring process robustness and reproducibility for long runs. While optimized specifically for the nitration of **1**, the system can also accommodate other 5-membered heteroaromatic substrates. The final demonstrator fully integrates the process from **1** to a small library of four marketed nitrofuran pharmaceuticals through advanced process concatenation.

Results and Discussion

Acetyl nitrate, the mixed anhydride of acetic and nitric acids, can be prepared according to different protocols.^[22–24] The safest and most convenient in situ protocol calls for premixing the desired substrate with either acetic acid and/or acetic anhydride before the addition of concentrated nitric acid, in the presence of a catalytic amount of sulfuric acid.^[15,26] Although these conditions have been reported for the nitration of furfural **1** in batch,^[27–29] the reaction lacks reproducibility due to the decomposition of the substrate.^[14]

We developed a continuous flow generator^[30] of acetyl nitrate from acetic anhydride and nitric acid with catalytic sulfuric acid using commercially available fluidic components (Figure 2) made from polymers of either perfluoroalkoxy alkane (PFA) or polytetrafluoroethylene (PTFE). To address the harsh, highly acidic reaction conditions, specifically

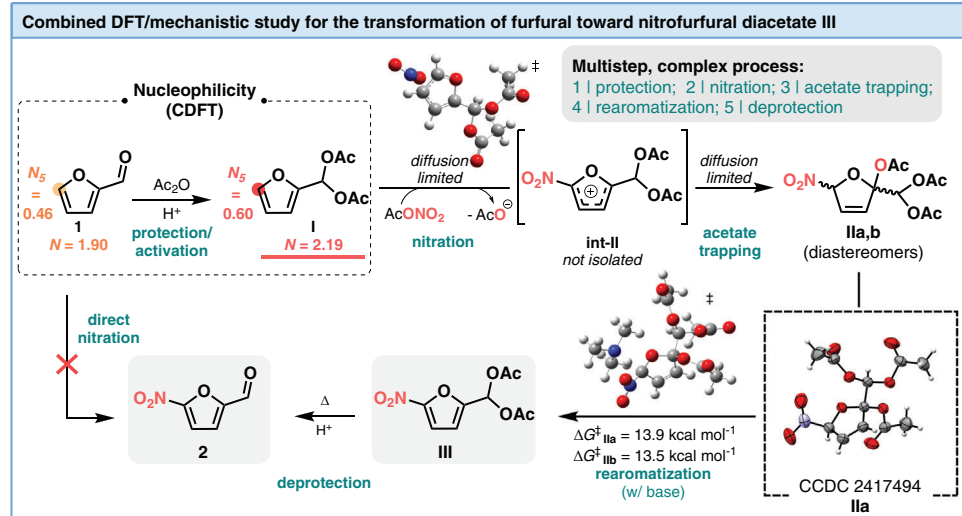


Figure 3. Nitration of furfural with acetyl nitrate (AcONO_2). Sequence of reaction steps and intermediates en route to nitrofurfural **2**. The structure of intermediate **IIa** was confirmed through XRD (Section S12, Supporting Information). Global and local nucleophilicities are indicated for compounds **1** and **I** (Section S8, Supporting Information) and are expressed in eV.^[35] The nitration of **I** was studied computationally with Gaussian 16^[31] (Section S8, Supporting Information) at the B3LYP-GD3B/6-31+G*/M08HX/6-311++G** level of theory (SMD = acetic anhydride, 273 K). The base-induced rearomatization was computed with Me_3N as a model Brønsted base (Section S8, Supporting Information).

designed chemically resistant ceramic pressure transducers were developed. To ensure the precise flow rate of the >90% nitric acid, the mass decrease of feed solution over time was monitored. In addition, an in-line IR module provided a convenient real-time monitoring system for steady state, with the characteristic vibration bands at $780\text{--}810\text{ cm}^{-1}$ (stretching) and $690\text{--}740\text{ cm}^{-1}$ (scissoring) (Figure 2).

The mechanism for the formation of acetyl nitrate, which was studied computationally (Section S8, Supporting Information), involves a diffusion-limited, two-step process. The first step involves the addition of a nitrate anion to protonated acetic anhydride and leads to the formation of an unstable intermediate (Figure 2). The latter decomposes with the concomitant release of acetic acid and the desired mixed anhydride. The optimized conditions for the formation of acetyl nitrate in the novel generator (G_1) use neat acetic anhydride (5 equiv. relative to HNO_3 , 0.82 mL min^{-1}) and fuming nitric acid (with 3 mol% concentrated sulfuric acid, 0.08 mL min^{-1}) with a residence time of 40 s at $15\text{ }^\circ\text{C}$ (Figure 2). The output of acetyl nitrate, assuming quantitative conversion, is 0.104 mol h^{-1} (daily productivity of 262 g).

With the optimum conditions for the formation of acetyl nitrate in hand, the direct nitration of **1** was next studied under flow conditions. As the deactivating aldehyde group of furfural hinders direct electrophilic aromatic substitution, the nitration of **1** is a rather complex network of reaction intermediates, which has been the subject of debate in the literature.^[32–34] One historical question has been whether **1** or furfural diacetate (**I**) is the species that is nitrated. Conceptual Density Functional Theory (CDFT) was used to assess the global nucleophilicity of **1** ($N = 1.90\text{ eV}$) and **I** ($N = 2.19\text{ eV}$), concluding that furfural diacetate (**I**) is more nucleophilic than **1** and therefore more suitable for fast nitration.^[35] This

is further strengthened with stronger local nucleophilicities at C-5 for **I** ($N_5 = 0.60$) than for **1** ($N_5 = 0.46$).

In solution, acetyl nitrate equilibrates into its ionic counterparts, allowing the formation of nitronium species.^[23] Computations indicated that the reaction of **I** with nitronium is diffusion limited, thus associated with extremely fast kinetics. As observed experimentally, this leads to the formation of nitrofurfural triacetate **II** as a mixture of diastereoisomers (**IIa,b**), with compound **III** as minor component. The latter observation indicated that, quite unexpectedly, the direct rearomatization of cationic intermediate **int-II** was not favored under these conditions. Instead, rearomatization occurred following base treatment on **IIa,b** through two diastereomeric pathways with slightly different activation barriers, both converging to **III**. These computational results align with literature reports and our own observations of different kinetic constants for these substrates (Figure 3).^[36]

We then addressed the conversion of neat **1** to **III** under flow conditions. The upstream acetyl nitrate generator (G_1) was fluidically connected in series to a downstream nitration module $R_{1,3}$ (Figure 4a and Section S7.4.2, Supporting Information). Pre-cooling loops were added to all feeds connected to G_1 and R_1 to improve robustness, as well as reproducibility. A DIY in-line UV cell, clipped outside the PFA tubing to prevent contact with the harsh reaction medium, was inserted downstream R_1 . The in-line UV cell monitored the relative changes in absorbance over time, thus providing insight into the stability of the continuous nitration reaction in real-time (Section S5.7, Supporting Information).

Preliminary results under flow conditions gave partial conversion of **1** to a mixture of furfural diacetate **I**, nitrofurfural triacetate **IIa,b**, nitrofurfural diacetate **III**, and trace amounts

1523-3773 (2025) 25: 25, Downloaded from https://onlinelibrary.wiley.com/doi/10.1002/anci.20251660 by Universiteitsbibliotheek Gent, Wiley Online Library on [21/08/2025]. See the Terms and Conditions (https://onlinelibrary.wiley.com/terms-and-conditions) on Wiley Online Library for rules of use; OA articles are governed by the applicable Creative Commons License

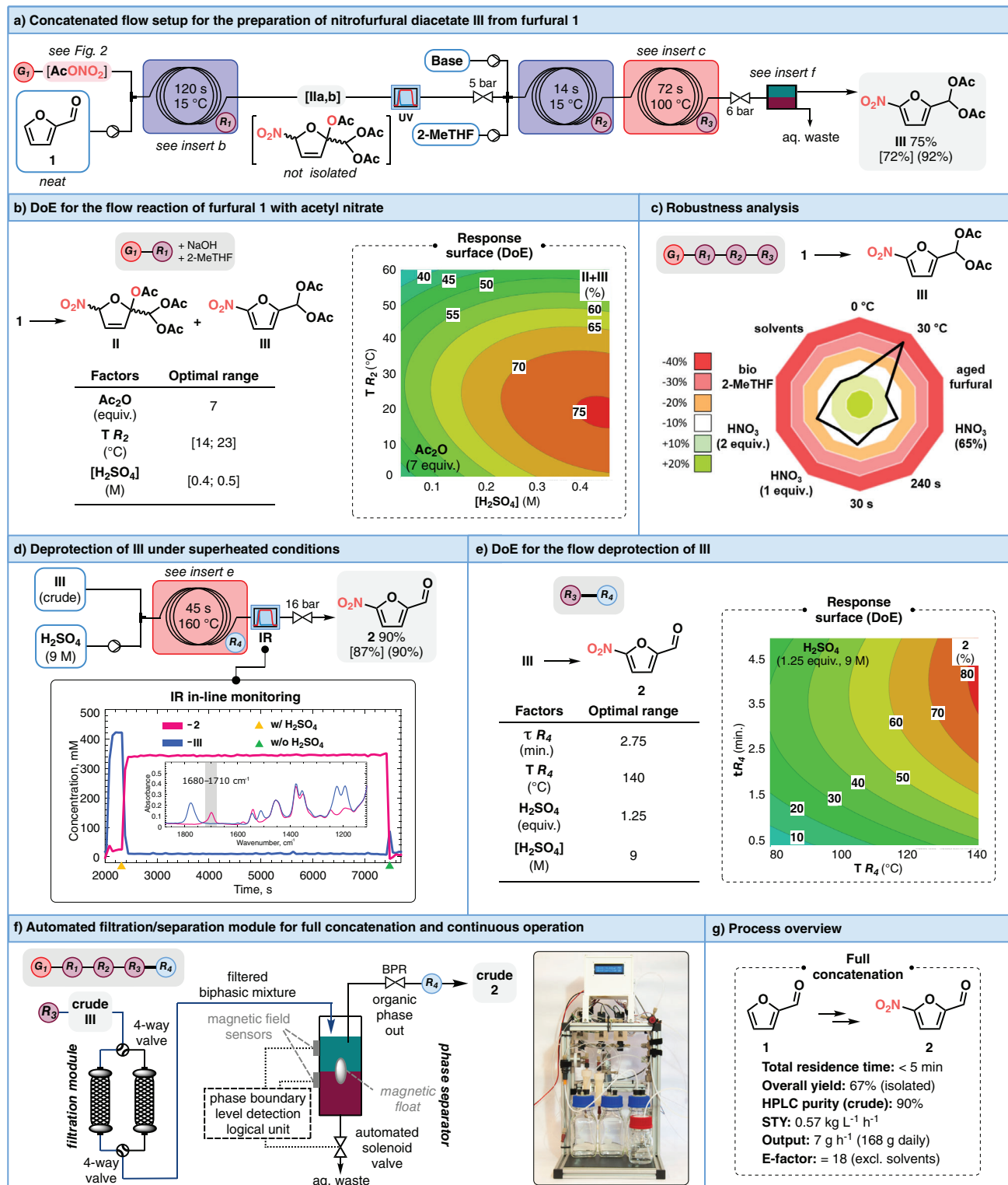


Figure 4. Optimization and robustness of the flow nitration platform. HPLC yields; isolated yields are in brackets; HPLC purities of isolated products are in parentheses. a) Simplified flow chart of the continuous flow setup for the nitration of furfural **1** toward intermediate **III**. b) Design of experiment (DoE) optimization response curve for the nitration of **1**. Data generated with 1.4 equiv. of HNO_3 (relative to **1**) and 2 min residence time in R_1 . All samples were processed using in-line quenching and extraction with 1 volume of 4 M NaOH (aq.) and 1 volume of 2-methyltetrahydrofuran (2 mL min^{-1} each). c) Robustness evaluation of the flow process. Data generated with deviations (OVAT) from the optimum conditions, including the concentration of nitric acid, the HNO_3/I stoichiometric ratio, the process temperature in R_1 , the residence time, the quality of furfural and the nature of the solvent. All samples were processed using in-line quenching and extraction with the concomitant injection of 1 volume of 6 M KOH (aq.) and 1 volume of an organic solvent. The organic solvent was typically 2-methyltetrahydrofuran (2-MeTHF) unless otherwise specified. d)

of **2**. To maximize the conversion of **1** and the combined yield of **II** + **III**, a design of experiment (DoE) approach was followed (Figure 4b). Three critical factors were identified: the excess of acetic anhydride, the concentration of sulfuric acid in nitric acid, and the operational temperature in R_1 (Section S7.4.2, Supporting Information).

Optimal parameters for the nitration reaction were identified as follows: for 1 equiv. of neat furfural **1**, 7 equiv. of neat acetic anhydride and 1.4 equiv. of HNO_3 (>90%) with 3 mol% H_2SO_4 (0.45 M solution) are needed to give full conversion of **1** under 2 min at 15 °C. These parameters led to 75% combined HPLC yield for **II** (50%) and **III** (20%), along with 5% of **2**. These conditions slightly reduce the excess of acetic anhydride compared to reported batch protocols.^[27–29] This excess could be further lowered (5 equiv.) though at the cost of decreasing the yield to 65%.

Subsequent work aimed at increasing the conversion of **IIa,b** into **III**. According to literature precedents in batch, adjustment of the pH to 2.5 is required, followed by heating the crude solution for at least 1 h to 55 °C.^[27–29] However, it was necessary to accelerate the rearomatization for the flow process. After multiple attempts (Section S7.4.3, Supporting Information), the concomitant injection of a 6 M KOH aqueous solution and 2-methyltetrahydrofuran was adopted, combined with an additional R_3 module operated at 100 °C. Under these conditions, complete conversion of **II** and total selectivity toward **III** were achieved within a residence time of 72 s. The optimized concatenated protocol (Figure 4a) was successfully repeated over 60 production campaigns ranging from 30 min to 4 h. It consistently delivered yields of $75 \pm 3\%$ (92% HPLC purity with ~5% of the desired **2** as major impurity) with a productivity of 53 mmol h⁻¹ (daily productivity of 307 g). In comparison, previously reported batch processes toward **III** typically achieved yields between 15% and 60%.^[37]

Robustness was evaluated using Glorius' approach^[38] to assess the impact of disturbances on key parameters (Figure 4c and Section S7.4.7, Supporting Information). Deviations included nitric acid concentration (65% vs >90%) and equivalents (1 or 2 equiv. versus 1.4 equiv.), R_1 temperature (0 °C or 30 °C vs 15 °C), residence time (30 s or 240 s vs 120 s), furfural freshness (5 + year-aged vs freshly distilled), and solvent type (THF, ethyl acetate, DCM or MEK vs 2-MeTHF). The study revealed minimal yield loss (0–10%) for most deviations, demonstrating robustness. Notably, using 65% instead of fuming HNO_3 proved safer, more affordable, and chemically more compatible, while skipping furfural distillation offered economic benefits. Flexibility in solvent choice for the extraction step by substituting biobased 2-MeTHF with other FDA-classified solvents, added practicality. The most critical parameter appeared to be the temperature at which R_1 was operated: at 30 °C

instead of 15 °C, the yield dropped significantly by 34%. This analysis complements the DoE and aligns with ICH Q13 guidelines, ensuring reproducibility for continuous API manufacturing.^[39]

The next step focused on the deacylation of **III**, to obtain deprotected nitrofurfural **2** (Figure 4d,e). This transformation is commonly reported under acidic conditions (both homogeneous and heterogeneous).^[27–29,40,41] Typical homogeneous batch conditions involve 50% H_2SO_4 at elevated temperatures (>100 °C). Preliminary experiments were performed with crude **III** in 2-MeTHF at high temperature under microwave irradiation using sulfuric acid, which resulted in extensive degradation (Section S7.2, Supporting Information). The deprotection was then transposed to flow chemistry using the crude output of **III** in 2-MeTHF collected from the previous step (Figure 4d) and optimized through DoE (Figure 4e). Deacylation of **III** to **2** and degradation were considered throughout the optimization round. Both these responses were interdependent and increased with (1) reaction time, (2) reaction temperature, (3) sulfuric acid equivalents, and (4) sulfuric acid concentration, leaving a very narrow optimization window. Following the DoE model (Figure 4e), the process was intensified using an elevated temperature of 160 °C. Total conversion (90% HPLC yield) was achieved within 45 s of residence time using 1.25 equiv. of H_2SO_4 as a 9 M solution (infused at 0.12 mL min⁻¹) (Section S7.4.8, Supporting Information).

One critical step in achieving full concatenation from **1** was the liquid–liquid extraction of **III** prior to diacetate deprotection (Figure 4f). Membrane separation was not implementable on the long term due to sporadic solid particle formation^[42,43]; gravity-based separation with optical detection of the interface was also very challenging due to the dark coloration of both phases.^[44] To address both challenges, an automated filtration/extraction unit was developed (Figure 4f), equipped with magnetic interfacial detection coupled with automated actuators and valves (Section S5.2, Supporting Information). Furthermore, temperature and pressure sensors were placed at critical positions to provide information on steady state, and any deviations from it. Furthermore, additional PAT (in-line FTIR, Figure 4d) was installed at the outlet of R_4 to monitor the final concentration of **2**.

Lastly, efforts to demonstrate the versatility of our nitration flow platform encompassed both expanding the scope to other 5-membered heteroaromatic substrates structurally akin to **1** and demonstrating the preparation of marketed APIs from **2** (Figure 5). For the scope of other heteroaromatic aldehydes, no further optimization was attempted. The optimal conditions for **1** were transposed to 3-furaldehyde **1'a**, thiophenecarboxaldehyde **1'b** and *N*-methyl-2-pyrrolecarboxaldehyde **1'c**, providing key intermediates for the preparation of various APIs such

Simplified flow chart of the continuous flow setup for the deacylation of nitrofurfural diacetate **III** toward **2**, emphasizing PAT with real-time, in-line IR reaction monitoring. e) Design of experiment (DoE) optimization response curve for the deacylation of intermediate **III**. All experiments were carried with crude **III** as a 0.39 M solution in 2-MeTHF (see also inserts a. and b.). After thermal quench, samples were diluted prior to HPLC analysis. f) Details on the automated filtration/separation unit that enables full concatenation of the process from **1** to **2** (Section S5.2, Supporting Information). g) Metrics for the fully concatenated process.

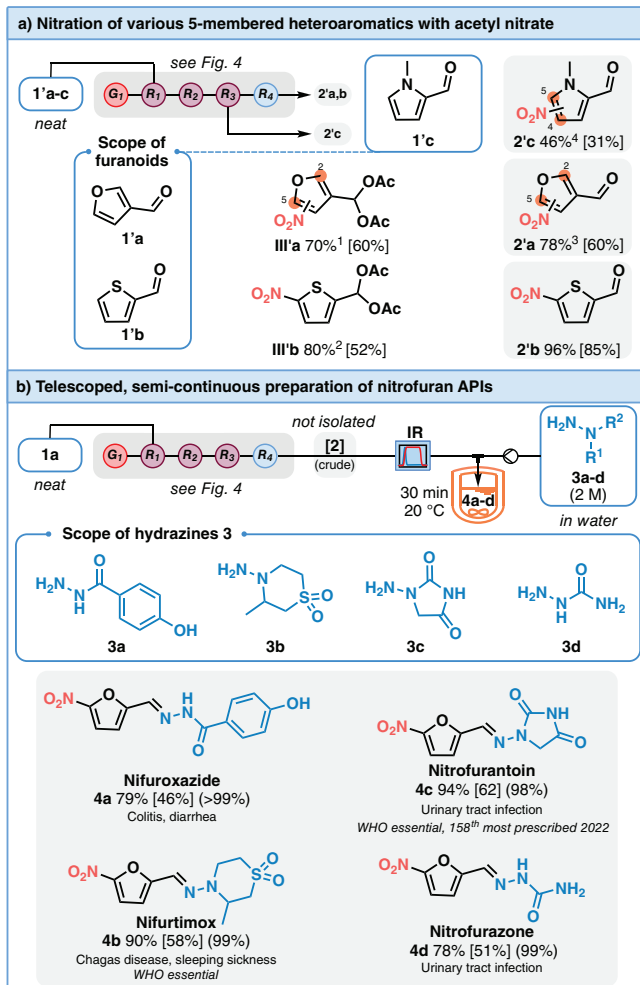


Figure 5. Versatility of the continuous flow nitration platform. HPLC yields; Overall isolated yields in brackets; HPLC purities are indicated in parentheses for compounds **4a-d**. a) Scope of the nitration platform on other heteroaryl aldehydes **1'a-c**. The conditions used are the same as for compound **1** (see Figure 4). ¹Compound **III'a** was obtained after **R**₃ as a 68:32 2-nitro/5-nitro regioisomeric mixture in 70% combined yield (full conversion). ²Compound **III'b** was obtained after **R**₃ as a single regioisomer in 80% yield. ³Compound **2'a** was obtained after **R**₄ as a mixture of 2-nitro and 5-nitro regioisomers in 78% combined yield. ⁴Compound **2'c** was obtained directly after **R**₃ as a 4:1 4-nitro/5-nitro regioisomeric mixture, while the deacylation already occurred in **R**₃. b) Use of the nitration platform for the preparation of 4 representative nitrofuran APIs (**4a-d**) through the coupling of crude **2** and a series of hydrazines **3a-d** (Section S7.4.11, Supporting Information). Nifurtimox **4b** was obtained through a slightly adapted protocol to accommodate its solubility (Section S7.4.12, Supporting Information).

as netropsin,^[45,46] distamycin,^[45,46] and 5-nitrothiophene semicarbazone antifungals and antitumors (Figure 5a).^[47,48] The preparation of marketed APIs from **2** was successfully achieved on a selection of best-selling nitrofurans (nifuroxazole **4a**, nifurtimox **4b**, nitrofurantoin **4c**, and nitrofurazone **4d**). To this end, the reactor effluent from **R**₄ was merged with a stream of hydrazines **3** (Figure 5b). In-line IR concentration monitoring of **2** (Figure 4d) allowed precise adjustment of the flow rates of **3** to maintain equimolarity. The corresponding stoichiometric mixtures were allowed

to react in a continuously stirred tank reactor (CSTR). The resulting hydrazones were filtered, washed and dried, yielding **4a-d** in 78–94% isolated yield (46–62% overall isolated yield from **1** over the three steps). The entire process is embedded with data acquisition tools, allowing in situ monitoring of its stability, including critical startup and shutdown procedures. The remote control of individual components is also implemented to ensure high safety and reproducibility of the results (Section S5.6, Supporting Information), fulfilling the aims of PAT. The system combining both nitration and deacylation was continuously operated for over 4 h, providing a space-time yield of 0.572 kg L⁻¹ h⁻¹ for **2**. This system provides a daily output of 261.4 g (98% HPLC purity) for nitrofurantoin **4c**, representing 5200 daily doses based on a 50 mg API dosage. Additionally, this process comes with a low E-factor of 18, pending the recycling of aqueous and organic effluents.

Conclusion

We present a highly automated, robust and safe acetyl nitrate generator designed for the nitration of delicate furan derivatives as intermediates for antibiotic and antibacterial nitrofuran production. This approach integrates the assets of flow chemistry, in-line data monitoring, and process analytical technology (PAT), whereas computational support provides insights for rationalizing reactivity. The upstream flow setup accommodates various heteroaromatics, while the downstream hydrazine coupling can be adapted to produce four market-leading nitrofuran active pharmaceutical ingredients, showcasing its versatility. Nitrofurantoin, one of the best-selling nitrofuran APIs, is obtained in 94% isolated yield (62% overall from furfural) in under 5 minutes. Favorable metrics are achieved through the use of neat feedstock solutions, water, biobased solvents, and widely available chemicals. The high level of integration and automation, featuring a newly developed filtration and liquid/liquid gravity separator unit, chemically resistant sensors and automated valves ensures robustness and reproducibility for this notoriously challenging sequence of reactions. Despite its complexity, the system remains manageable by a single operator and is adaptable for a range of reactions without reconfiguration. This innovative platform significantly reduces reaction time and enhances safety, offering a valuable tool for synthesizing important nitrated compounds in line with modern pharmaceutical industry standards.

Supporting Information

The Supporting Information is available free of charge: Methods, hardware, experimental protocols, analytical data, and computational data (PDF). All details, as well as the instructions for pressure transducers, electrically actuated valves, devices for pressure and temperature measurement (PTMB), the software for pressure and temperature acquisition, the nitric acid dosing controller, the filtration and separation module control unit (FSMCU) including a continuous-flow gravity separator with magnetic phase boundary tracking, the

UV-Vis flow cell and the furfural nitration data acquisition and process control software are provided free of charge on GitHub (<https://github.com/CiTOS-ULiege/Tools-for-Flow-Chemistry.git>) and Zenodo with the following <https://doi.org/10.5281/zenodo.15106903>. The authors have cited additional references within the Supporting Information.^[49–63]

Acknowledgements

This research was supported by the U.S. Food and Drug Administration under the FDA BAA-22-00123 program, Award Number 75F40122C00192. The authors acknowledge the University of Liège and the “Fonds de la Recherche Scientifique de Belgique (F.R.S.-FNRS)” (Incentive grant for scientific research MIS under grant No F453020F, JCMM). Computational resources were provided by the “Consortium des Équipements de Calcul Intensif (CÉCI)”, funded by the F.R.S.-FNRS under Grant No. 2.5020.11 and by the Walloon Region. The authors thank Dr. Cedric Malherbe (ULiège) for his help processing the in-line PAT-FTIR data. KVH thanks the Special Research Fund (BOF)–UGent (project: BOF/24J/2023/084).

Conflict of Interests

The authors declare no conflict of interest.

Data Availability Statement

The data that support the findings of this study are available in the supplementary material of this article.

Keywords: Flow chemistry • Furfural • Nitration platforms • Nitrofurans • Process analytical technology

- [1] G. Booth, in *Ullmann's Encyclopedia of Industrial Chemistry*, Wiley, Weinheim, Germany **2000**, https://doi.org/10.1002/14356007.a17_411.
- [2] K. M. Aitken, in *Science of Synthesis: Houben–Weyl Methods of Molecular Transformations* (Eds.: C. A. Ramsden, D. Bellus), Georg Thieme Verlag, Stuttgart **2007**, pp. 1183–1320.
- [3] H. K. Porter, in *Organic Reactions*, Wiley, Hoboken, NJ **2011**, pp. 455–481.
- [4] T. Kahl, K.-W. Schröder, F. R. Lawrence, W. J. Marshall, H. Höke, R. Jäckh, in *Ullmann's Encyclopedia of Industrial Chemistry*, Wiley-VCH Verlag GmbH & Co. KGaA, Weinheim, Germany **2000**.
- [5] T. L. Guggenheim, (ed.), in *Chemistry*, American Chemical Society, Washington, DC **2013**.
- [6] P. G. Urben, (ed.), in *Bretherick's Handbook of Reactive Chemical Hazards*, Elsevier, Amsterdam **2017**, C1 pp. 81–882.
- [7] S. G. Newman, K. F. Jensen, *Green Chem.* **2013**, *15*, 1456.
- [8] J. Tibhe, Y. Sharma, R. A. Joshi, R. R. Joshi, A. A. Kulkarni, *Green Process. Synth.* **2014**, *3*, 279–285.
- [9] C. E. Brocklehurst, H. Lehmann, L. La Vecchia, *Org. Process Res. Dev.* **2011**, *15*, 1447–1453.
- [10] Q. Song, X. Lei, S. Yang, S. Wang, J. Wang, J. Chen, Y. Xiang, Q. Huang, Z. Wang, *Molecules* **2022**, *27*, 5139.
- [11] I. Castillo, J. Rehrl, P. Sagmeister, R. Lebl, J. Kruisz, S. Celikovic, M. Sipek, D. Kirschneck, M. Horn, S. Sacher, D. Cantillo, J. D. Williams, J. G. Khinast, C. O. Kappe, *J. Process Contr.* **2023**, *122*, 59–68.
- [12] D. Cantillo, M. Damm, D. Dallinger, M. Bauser, M. Berger, C. O. Kappe, *Org. Process Res. Dev.* **2014**, *18*, 1360–1366.
- [13] S. Patra, I. Mosiagin, R. Giri, D. Katayev, *Synthesis* **2022**, *54*, 3432–3472.
- [14] G. A. Olah, R. Malhotra, S. C. Narang, in *Nitration: Methods and Mechanisms*, VCH: Weinheim, Germany **1989**.
- [15] M. Köckinger, B. Wyler, C. Aellig, D. M. Roberge, C. A. Hone, C. O. Kappe, *Org. Process Res. Dev.* **2020**, *24*, 2217–2227.
- [16] J. Pelleter, F. Renaud, *Org. Process Res. Dev.* **2009**, *13*, 698–705.
- [17] J. W. Döbereiner, *Annalen der Pharmacie* **1832**, *3*, 141–146.
- [18] F. N. Peters, *Ind. Eng. Chem.* **1936**, *28*, 755–759.
- [19] J. J. Bozell, G. R. Petersen, *Green Chem.* **2010**, *12*, 539.
- [20] P.-S. Chu, M. I. Lopez, A. Abraham, K. R. El Said, S. M. Plakas, *J. Agric. Food. Chem.* **2008**, *56*, 8030–8034.
- [21] M. L. Bouveault, M. A. Wahl, *C. R. Hebd. Séances Acad. Sci.* **1902**, *134*, 776–777.
- [22] H. Burton, P. F. G. Praill, *J. Chem. Soc.* **1955**, 729.
- [23] R. Louw, in *Encyclopedia of Reagents for Organic Synthesis*, John Wiley & Sons, Ltd, Chichester, UK **2001**.
- [24] A. Chrétien, G. Boh, “Le nitrate d’acétyl agent de synthèse pour la préparation des nitrates minéraux anhydres,” can be found under <https://gallica.bnf.fr/ark:/12148/bpt6k3172c/f822.item.2025>.
- [25] H. C. Leung, T. C. Lee, W. Wong, W. C. Fu, *Adv. Synth. Catal.* **2024**, *366*, 4385–4391.
- [26] G. Panke, T. Schwalbe, W. Stirner, S. Taghavi-Moghadam, G. Wille, *Synthesis* **2003**, 2827–2830.
- [27] H. Jin, Y. Geng, Z. Yu, K. Tao, T. Hou, *Pestic. Biochem. Physiol.* **2009**, *93*, 133–137.
- [28] S. M. Taimoory, S. I. Sadraei, R. A. Fayoumi, S. Nasri, M. Revington, J. F. Trant, *J. Org. Chem.* **2018**, *83*, 4427–4440.
- [29] G. A. Gamov, A. N. Kiselev, A. E. Murekhina, M. N. Zavalishin, V. V. Aleksandriiskii, D. Y. Kosterin, *J. Mol. Liq.* **2021**, *341*, 116911.
- [30] D. Dallinger, B. Gutmann, C. O. Kappe, *Acc. Chem. Res.* **2020**, *53*, 1330–1341.
- [31] Gaussian 16, Revision C.01, M. J. Frisch, G. W. Trucks, H. B. Schlegel, G. E. Scuseria, M. A. Robb, J. R. Cheeseman, G. Scalmani, V. Barone, G. A. Petersson, H. Nakatsuji, X. Li, M. Caricato, A. V. Marenich, J. Bloino, B. G. Janesko, R. Gomperts, B. Mennucci, H. P. Hratchian, J. V. Ortiz, A. F. Izmaylov, J. L. Sonnenberg, D. Williams-Young, F. Ding, F. Lipparini, F. Egidi, J. Goings, B. Peng, A. Petrone, T. Henderson, D. Ranasinghe, et al. Gaussian, Inc., Wallingford, CT **2019**.
- [32] H. Gilman, G. F. Wright, *J. Am. Chem. Soc.* **1930**, *52*, 4165–4166.
- [33] J. G. Michels, K. J. Hayes, *J. Am. Chem. Soc.* **1958**, *80*, 1114–1116.
- [34] A. Gaset, J. P. Gorrichon, *Org. Magn. Reson.* **1981**, *16*, 239–241.
- [35] M. Ríos-Gutiérrez, A. Saz Sousa, L. R. Domingo, *J. Phys. Org. Chem.* **2023**, *36*, e4503.
- [36] G. Balina, P. Kesler, J. Petre, P. Dung, A. Vollmar, *J. Org. Chem.* **1986**, *51*, 3811–3818.
- [37] A. R. Katritzky, E. F. V. Scriven, S. Majumder, R. G. Akhmedova, N. G. Akhmedov, A. V. Vakulenko, *Arkivoc* **2005**, *2005*, 179–191.
- [38] F. Schäfer, L. Lückemeier, F. Glorius, *Chem. Sci.* **2024**, *15*, 14548–14555.
- [39] “ICH guideline Q13 on continuous manufacturing of drug substances and drug products” can be found under <https://www.ich.org/page/quality-guidelines> (accessed: January 2025).
- [40] R. Pal, T. Sarkar, S. Khasnabis, *Arkivoc* **2012**, *2012*, 570–609.

[41] L. N. Palacios-Grijalva, D. Y. Cruz-González, L. Lomas-Romero, E. González-Zamora, G. Ulibarri, G. E. Negrón-Silva, *Molecules* **2009**, *14*, 4065–4078.

[42] B. Liang, X. He, J. Hou, L. Li, Z. Tang, *Adv. Mater.* **2019**, *31*, 1806090.

[43] A. Adamo, P. L. Heider, N. Weeranoppanant, K. F. Jensen, *Ind. Eng. Chem. Res.* **2013**, *52*, 10802–10808.

[44] A. Adamo, R. L. Beingessner, M. Behnam, J. Chen, T. F. Jamison, K. F. Jensen, J.-C. M. Monbaliu, A. S. Myerson, E. M. Revalor, D. R. Snead, T. Stelzer, N. Weeranoppanant, S. Y. Wong, P. Zhang, *Science* **2016**, *352*, 61–67.

[45] Y. Yamamoto, T. Kimachi, Y. Kanaoka, S. Kato, K. Bessho, T. Matsumoto, T. Kusakabe, Y. Sugiura, *Tetrahedron Lett.* **1996**, *37*, 7801–7804.

[46] A. I. Khalaf, R. D. Waigh, A. J. Drummond, B. Pringle, I. McGroarty, G. G. Skellern, C. J. Suckling, *J. Med. Chem.* **2004**, *47*, 2133–2156.

[47] L. L. N. de Araújo Neto, M. do Carmo Alves de Lima, J. F. de Oliveira, E. R. de Souza, M. D. S. Buonafina, M. N. Vitor Anjos, F. A. Brayner, L. C. Alves, R. P. Neves, F. J. B. Mendonça-Junior, *Chem.-Biol. Interact.* **2017**, *272*, 172–181.

[48] K. M. Roque Marques, M. R. do Desterro, S. M. de Arruda, L. N. de Araújo Neto, M. do Carmo Alves de Lima, S. M. V. de Almeida, E. C. D. da Silva, T. M. de Aquino, E. F. da Silva-Júnior, J. X. de Araújo-Júnior, M. M. de Silva, M. D. A. de Dantas, J. C. C. Santos, I. M. Figueiredo, M.-A. Bazin, P. Marchand, T. G. da Silva, F. J. B. Mendonça-Junior, *Curr. Top. Med. Chem.* **2019**, *19*, 1075–1091.

[49] Rigaku Oxford Diffraction, in *CrysAlisPro Software system, version 1.171.42*. Vol. 49, Rigaku Corporation, Oxford, UK **2022**.

[50] O. V. Dolomanov, L. J. Bourhis, R. J. Gildea, J. A. K. Howard, H. Puschmann, *J. Appl. Crystallogr.* **2009**, *42*, 339–341.

[51] G. M. Sheldrick, *Acta Crystallogr. Sect. A* **2015**, *A71*, 3–8.

[52] G. M. Sheldrick, *Acta Crystallogr. Sect. A* **2015**, *C71*, 3–8.3.

[53] P. K. Kancharla, Y. S. Reddy, S. Dharuman, Y. D. Vankar, *J. Org. Chem.* **2011**, *76*, 5832–5837.

[54] M. R.-G. Domingo, P. Pérez, *Molecules* **2016**, *21*, 748.

[55] A. V. Yarkov, “5-nitro-2-thiophenemethanediol diacetate,” can be found under <https://spectrabase.com/compound/9NDyHj4FUkQ#JXr4JoAYowY> (accessed: January 2025).

[56] G. Aridoss, K. K. Laali, *J. Org. Chem.* **2011**, *76*, 8088–8094.

[57] C. Gallardo-Garrido, Y. Cho, J. Cortés-Rios, D. Vasquez, C. D. Pessoa-Mahana, R. Araya-Maturana, H. Pessoa-Mahana, M. Faundez, *Toxicol. Appl. Pharmacol.* **2020**, *401*, 115104.

[58] M. de la Concepción Foces-Foces, F. H. Cano, R. M. Claramunt, A. Fruchier, J. Elguero, *Bull. Soc. Chim. Belg.* **1988**, *97*, 1055–1066.

[59] L. Wechteti, N. H. Mekni, M. Romdhani-Younes, *Heterocycl. Comm.* **2018**, *24*, 187–191.

[60] M. Romdhani-Younes, M. M. Chaabouni, *J. Sulfur Chem.* **2012**, *33*, 223–228.

[61] M. Jereb, *Green Chem.* **2012**, *14*, 3047.

[62] L. Brard, R. J. Singh, K. K. Kwang, G. Saulnier-Sholler, US8193180, **2012**.

[63] H. Herlinger, K.-H. Mayer, (Bayer-AG), DE1670840A1, **1967**.

Manuscript received: January 20, 2025

Revised manuscript received: April 01, 2025

Accepted manuscript online: April 02, 2025

Version of record online: May 08, 2025